
Article:
Ellington, M., Martin, C. and Wang, B. (2024) Revisiting real wage rigidity. Journal of Money, Credit and Banking, 56 (2-3). pp. 613-626. ISSN 0022-2879

https://doi.org/10.1111/jmcb.13056

Revisiting Real Wage Rigidity
Online Appendix

Michael Ellington Chris Martin Bingsong Wang

October 21, 2022

1 Data

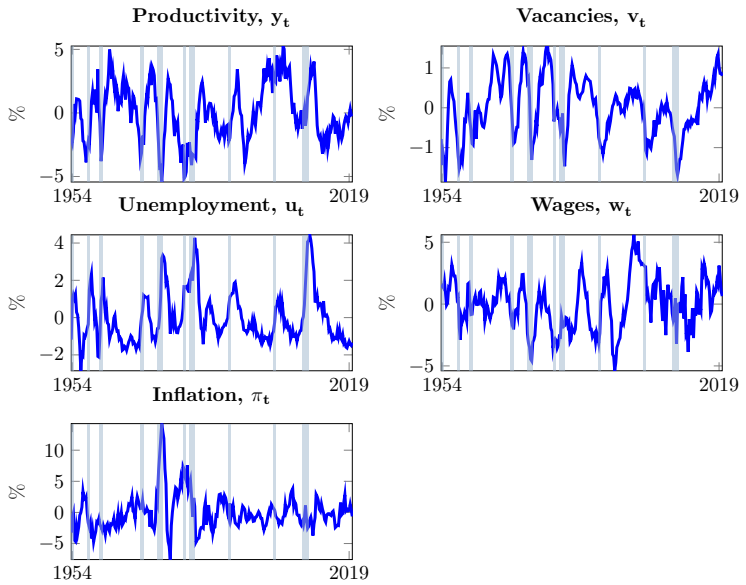

Figure 1: **US Macroeconomic data from 1954Q3 to 2019Q4**
Notes: This figure plots US labour market data from 1954Q3 to 2019Q4. The top left panel plots the log-levels of productivity, y_t; the top right panel plots the vacancy rate, v_t; the middle left panel plots the unemployment rate, u_t; the middle right panel plots the log-levels of the real wage, w_t; the bottom left panel plots the annual inflation rate, π_t. Grey bars indicate NBER recession dates. All variables have been filtered using the Hamilton (2018) filter.

2 Econometric Methodology

Our prior specification involves estimating a Bayesian fixed coefficient VAR (BVAR) model over the training sample. The priors imposed on this BVAR model combine the traditional Minnesota prior of Doan et al. (1984) and Litterman (1986) on the coefficient matrices with an inverse-Wishart prior on the BVAR's covariance matrix. In our specification, the prior mean on the coefficient matrix sets all elements equal zero, except those corresponding to the own first lag of each dependent variable which are set to 0.9. This imposes the prior belief that our variables exhibit persistence whilst simultaneously ensuring shrinkage of the other VAR coefficients to zero. The prior variance of the coefficient matrix is set similar to Litterman (1986). Our prior for the BVAR's covariance matrix follows an inverse-Wishart distribution with the prior scale matrix and degrees of freedom set to an N-dimensional identity matrix and 1+N respectively.

We estimate the BVAR using a standard Gibbs sampler. For the sake of brevity, we do not explicitly outline our algorithm since it is well documented; see e.g. Koop and Korobilis (2010). Our alternative prior specification essentially replaces the conventional Cogley and Sargent (2005) prior with the posterior means from the draws of an estimated BVAR over the training sample

$$\bar{\theta}_{\text{BVAR}} = \frac{1}{M}\sum_{i=1}^{M}\theta_i, \tag{1}$$

$$\overline{\text{V}(\theta)}_{\text{BVAR}} = \frac{1}{M}\sum_{i=1}^{M}\text{V}(\theta_i), \tag{2}$$

$$\bar{\Sigma}_{\text{BVAR}} = \frac{1}{M}\sum_{i=1}^{M}\Sigma_i \tag{3}$$

respectively. Here M denotes the number of saved draws from the estimated BVAR which we set to 20,000. θ_i and $\text{V}(\theta_i)$ denote the ith draw of the coefficient matrix and the variance of the coefficient matrix respectively. Σ_i denotes the ith draw of the BVAR's covariance matrix. From these estimates, the initial conditions of the time-varying coefficient models, θ_0, a_0, h_0 are Normal and independent of one another, and the distributions of the hyperparameters. We set

$$\theta_0 \backsim N\left[\bar{\theta}_{\text{BVAR}},\ 4\cdot\overline{\text{V}(\theta)}_{\text{BVAR}}\right] \tag{4}$$

for α_0, h_0, let $\bar{\Sigma}_{\text{BVAR}}$ be the estimated covariance matrix of the residuals from the time–invariant BVAR. Let C be the lower–triangular Choleski factor such that $CC' = \bar{\Sigma}_{\text{BVAR}}$. The prior for the stochastic volatilities are

$$\ln h_0 \backsim N(\ln \mu_0, 10 \times I_5) \tag{5}$$

where μ_0 collects the logarithms of the squared elements along the diagonal of C. Each column of C is divided by the corresponding element on the diagonal; call this matrix $\tilde{C}$. The prior for the

contemporaneous relations is

$$\alpha_0 \backsim N\left[\tilde{\alpha}_0,\ \tilde{V}(\tilde{\alpha}_0)\right] \tag{6}$$

with $\tilde{\alpha}_0 \equiv [\tilde{\alpha}_{0,11},\ \tilde{\alpha}_{0,21},\ \ldots,\ \tilde{\alpha}_{0,51}]'$ which is a vector collecting all the elements below the diagonal of $\tilde{C}^{-1}$. $\tilde{V}(\tilde{\alpha}_0)$ is diagonal with each element equal to 10 times the absolute value of the corresponding element of $\tilde{\alpha}_0$. This is an arbitrary prior but correctly scales the variance of each element of α_0 to account for their respective magnitudes.

For the time-varying coefficient model assuming $Q_t = Q$, we set Q to follow an inverse Wishart distribution.

$$Q \backsim IW(\underline{Q}^{-1}, \mathrm{T}_0) \tag{7}$$

where $\underline{Q} = (1 + \dim(\theta_t)) \cdot \overline{\mathrm{V}}(\bar{\theta}_{\mathrm{BVAR}}) \cdot 3.4 \times 10^{-4}$. The prior degrees of freedom, $(1 + \dim(\theta_t))$, are the minimum allowed for the prior to be proper. Our choice of scaling parameter of 3.4×10^{-4} is consistent with Cogley and Sargent (2005). We have also estimated our models using different priors, we allowed for a more restrictive scaling parameter of 1.0×10^{-4} and have also set the degrees of freedom to be the length of the training sample; in our case this is 80. The scaling parameter essentially sets the amount of drift within the θ matrices.

With regards to the hyperparameters under the assumption $Q_t = Q_t$, the diagonal elements of Q_t follow a geometric random walk, let $C_{\overline{\mathrm{V}(\bar{\theta}_{\mathrm{BVAR}})}}$ be the lower-triangular Choleski factor such that $C_{\overline{\mathrm{V}(\bar{\theta}_{\mathrm{BVAR}})}} C'_{\overline{\mathrm{V}(\bar{\theta}_{\mathrm{BVAR}})}} = 3.4 \times 10^{-4} \overline{\mathrm{V}(\bar{\theta}_{\mathrm{BVAR}})}$. We then set

$$\ln q_0 \backsim N\left[\ln \mu_{q_0,0}, 10 \times I_{\dim(\theta_t)}\right] \tag{8}$$

with $\ln \mu_{q_0,0}$ collecting the logarithmic squared diagonal elements of $3.4 \times 10^{-4} \overline{\bar{\theta}_{\mathrm{BVAR}})}$. The variances of these stochastic volatility innovations follow an inverse-Gamma distribution for the elements of Z_q,

$$Z_{q,i,i} \backsim IG(\frac{10^{-4}}{2},\ \frac{1}{2}) \tag{9}$$

The blocks of S are also assumed to follow inverse–Wishart distributions with prior degrees of freedom equal to the minimum allowed (i.e. $1 + \dim(S_i)$).

$$S_1 \backsim IW(\underline{S}_1^{-1}, 2) \tag{10}$$

$$S_2 \backsim IW(\underline{S}_2^{-1}, 3) \tag{11}$$

$$S_3 \backsim IW(\underline{S}_3^{-1}, 4) \tag{12}$$

$$S_4 \backsim IW(\underline{S}_4^{-1}, 5) \tag{13}$$

we set S_1, S_2, S_3 in accordance with $\tilde{\alpha}_0$ such that $\underline{S}_1 = 10^{-3} \times |\tilde{\alpha}_{0,21}|$, $\underline{S}_2 = 10^{-3} \times \mathrm{diag}([|\tilde{\alpha}_{0,31}|, |\tilde{\alpha}_{0,32}|]')$, $\underline{S}_3 =$

$10^{-3}\times$ diag($[|\tilde{\alpha}_{0,41}|,\ |\tilde{\alpha}_{0,42}|,\ |\tilde{\alpha}_{0,43}|]'$), $\underline{S}_4 = 10^{-3}\times$ diag($[|\tilde{\alpha}_{0,51}|,\ |\tilde{\alpha}_{0,52}|,\ |\tilde{\alpha}_{0,53}|,\ |\tilde{\alpha}_{0,54}|]'$). This calibration is consistent with setting S_1, S_2, S_3, S_4 to 10^{-4} times the corresponding diagonal block of $\tilde{V}(\tilde{\alpha}_0)$. The variances for the stochastic volatility innovations, as in Cogley and Sargent (2005), follow an inverse–Gamma distribution for the elements of W,

$$W_{i,i} \backsim IG(\frac{10^{-4}}{2},\ \frac{1}{2}) \tag{14}$$

In order to simulate the posterior distribution of the hyperparameters and states, conditional on the data, we implement the following MCMC that combines elements from Primiceri (2005) and Cogley and Sargent (2005).

1) *Draw elements of* θ_t Conditional on Y^T, α^T and H^T, the observation equation (1) is linear with Gaussian innovations with a known covariance matrix. Factoring the density of θ_t, $p(\theta_t)$ in the following manner

$$p(\theta^T|y^T, A^T, H^T, V) = p(\theta_T|Y^T, A^T, H^T, V) \prod_{t=1}^{T-1} p(\theta_t|\theta_{t+1}, Y^t, A^T, H^T, V) \tag{15}$$

the Kalman filter recursions pin down the first element on the right hand side of the above in the following manner: $p(\theta_T|Y^T, A^T, H^T, V) \backsim N(\theta_T, P_T)$, P_T is the precision matrix of θ_T from the Kalman filter. The remaining elements in the factorisation are obtained via backward recursions as in Cogley and Sargent (2005). Since θ_t is conditionally Normal

$$\theta_{t|t+1} = P_{t|t}P^{-1}_{t+1|t}(\theta_{t+1} - \theta_t) \tag{16}$$

$$P_{t|t+1} = P_{t|t} - P_{t|t}P^{-1}_{t+1|t}P_{t|t} \tag{17}$$

which yields, for every t from $T-1$ to 1, the remaining elements in the observation equation (1). More precisely, the backward recursion begins with a draw, $\tilde{\theta}_T$ from $N(\theta_T,\ P_T)$. Conditional on $\tilde{\theta}_T$, the above produces $\theta_{T-1|T}$ and $P_{T-1|T}$. This permits drawing $\tilde{\theta}_{T-1}$ from $N(\theta_{T-1|T},\ P_{T-1|T})$ until t=1.

2) *Drawing elements of* α_t Conditional on Y^T, θ^T and H^T we follow Primiceri (2005) and note that (1) can be written as

$$A_t\tilde{Y}_t \equiv A_t(Y_t - X_t'\theta_t) = A_t\epsilon_t \equiv \psi_t \tag{18}$$

$$Var(\psi_t) = H_t \tag{19}$$

with $\tilde{Y}_t \equiv [\tilde{Y}_{1,t},\ \tilde{Y}_{2,t},\ \tilde{Y}_{3,t},\ \tilde{Y}_{4,t}]'$ and

$$\tilde{Y}_{1,t} = \psi_{1,t} \tag{20}$$
$$\tilde{Y}_{2,t} = -\alpha_{21,t}\tilde{Y}_{1,t} + \psi_{2,t} \tag{21}$$
$$\tilde{Y}_{3,t} = -\alpha_{31,t}\tilde{Y}_{1,t} - \alpha_{32,t}\tilde{Y}_{2,t} + \psi_{3,t} \tag{22}$$
$$\tilde{Y}_{4,t} = -\alpha_{41,t}\tilde{Y}_{1,t} - \alpha_{42,t}\tilde{Y}_{2,t} - \alpha_{43,t}\tilde{Y}_{3,t} + \psi_{4,t} \tag{23}$$

These observation equations and the state equation permit drawing the elements of α_t equation by equation using the same algorithm as above; assuming S is block diagonal.

3) *Drawing elements of* H_t Conditional on Y^T, θ^T and α^T, the orthogonal innovations u_t, $Var(\psi_t) = H_t$ are observable. Following Jacquier et al. (2002) the stochastic volatilities, $h_{i,t}$'s, are sampled element by element; Cogley and Sargent (2005) provide details in Appendix B.2.5 of their paper.

4) *Drawing the hyperparameters* Conditional on Y^T, θ^T, H_t and α^T, the innovations in θ_t, α_t and $h_{i,t}$'s are observable, which allows one to draw the elements of $Q_t = Q$, S_1, S_2, S_3 and the $W_{i,i}$.

Note that for the model allowing for stochastic volatility in the innovation variances of the time-varying coefficients, Q_t being a diagonal matrix, we add an extra block into the MCMC algorithm.

3a) *Drawing the elements of* Q_t Conditional on θ_t, the innovations $\kappa_t = \theta_t - \theta_{t-1}$, with $\text{Var}(\kappa_t) = Q_t$ are observable. Therefore we sample the diagonal elements of Q_t applying the Jacquier et al. (2002) algorithm element by element. Following this, we can then sample the $Z_{q,i,i}$ from the inverse-Gamma distribution in step 4 of the above algorithm.

3 Reduced-Form Results

The upper panel of Figure 2 plots the posterior median and 80% highest posterior density intervals for the logarithmic determinant of the time-varying covariance matrices. The lower panel of Figure 2 plots the stochastic volatilities of each variable. Figure 3) contains the reduced-form correlations between our variables

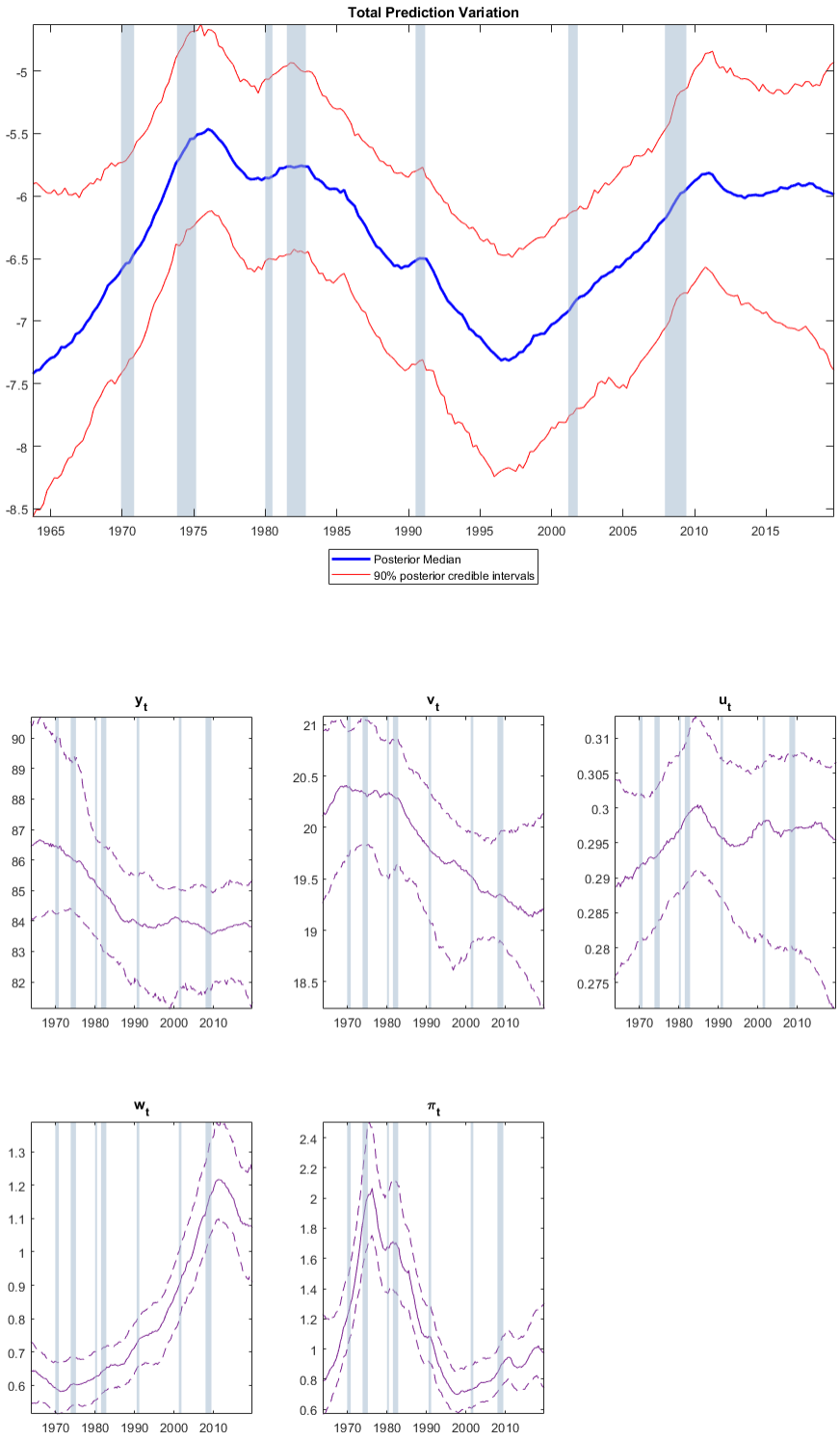

Figure 2: **Total Prediction Variation, $\ln|\Omega_{t|T}|$, and Stochastic Volatilities of US Labour Market Variables from 1964Q3 to 2016Q4**

Notes: The upper panel plots the posterior median, and 80% posterior credible intervals of logarithmic determinant of the time-varying reduced-form covariance matrices, $\ln|\Omega_{t|T}|$, from 1964Q3–2016Q4. The lower panel plots the posterior median, and 80% posterior credible intervals of the reduced-from stochastic volatility innovations of productivity, y_t (top left panel); real wages, w_t (top middle panel); the vacancy rate, v_t (top right panel); the unemployment rate, u_t (bottom left panel); and inflation, π_t (bottom middle panel) from 1964Q3–2016Q4. Grey bars indicate NBER recession dates.

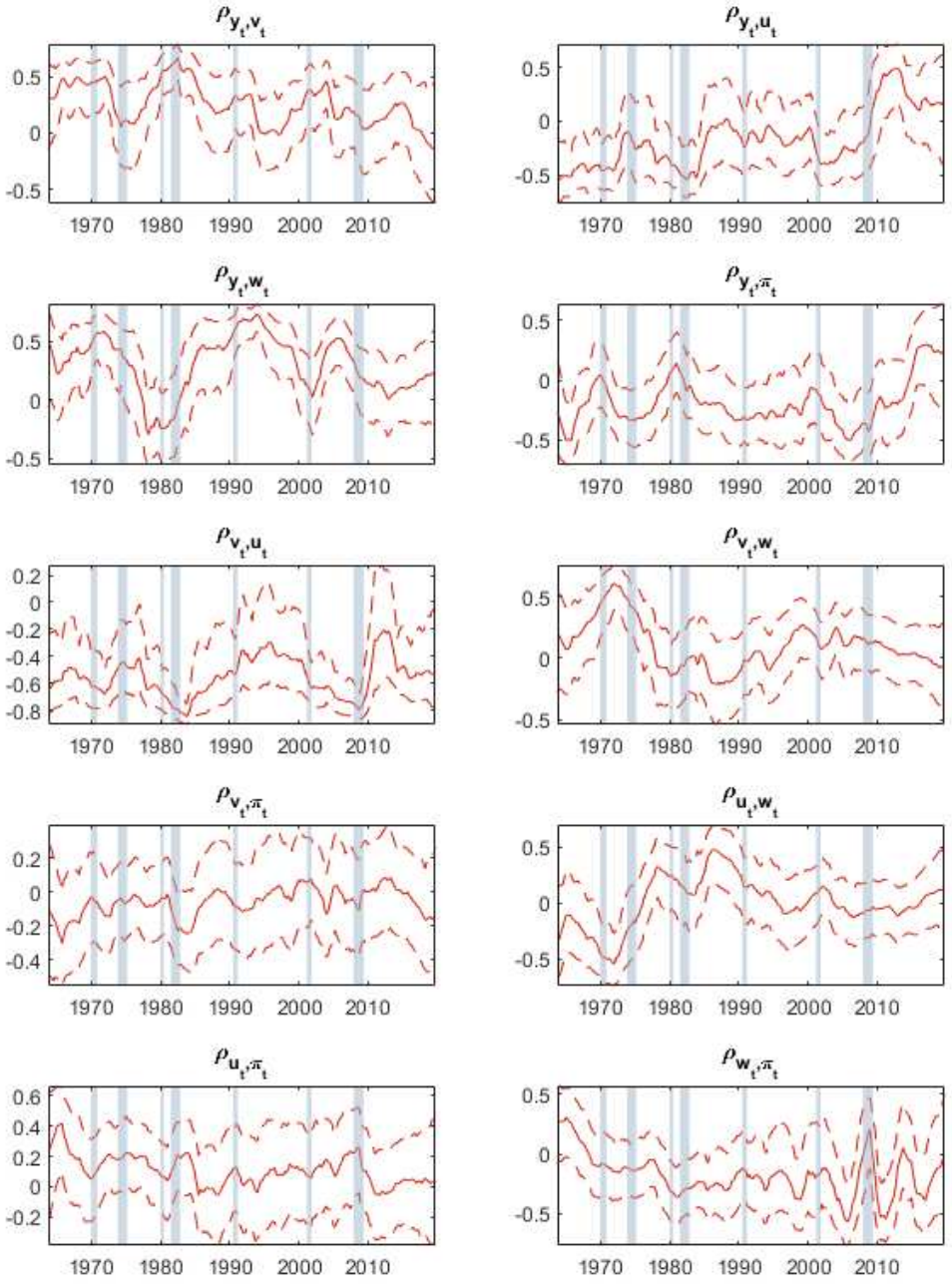

Figure 3: **Reduced-form correlations from 1964Q3 to 2019Q4**
Notes: This figure plots the posterior median, and 80% posterior credible intervals of the reduced-from model implied correlations of variables within the TVP VAR model from 1962Q1–2019Q4. $\hat{\rho}_{i_t,j_t}$ denotes the model implied correlation of variable i and j at time t respectively. y_t, w_t v_t, u_t, π_t denote productivity, real wages, the vacancy rate, the unemployment rate, and inflation, respectively. Grey bars indicate NBER recession dates.

4 Strategy for Identification of Structural Shocks

In this section we outline our identification strategy, which follows Canova and Paustian (2011) and Mumtaz and Zanetti (2015). We simulate a theoretical model using a range of alternative calibrations, based on randomly sampling parameter values within a specified range, constructing a distribution of impulse responses of our endogenous variables to a variety of shocks. We identify structural shocks for which the sign of the impulse responses on impact is unambiguous across this distribution. In this way, we ensure that our identifying sign restrictions are credible, robust to alternative calibrations of the structural parameters. Our identifying restrictions are based on a standard New Keynesian DSGE model without capital but with search frictions in the labour market, similar to Mumtaz and Zanetti (2012) and others.

We summarise the model and structural parameters in the upper panel of Table 1. Equations (T.1)–(T.6) outline the structure of the labour market. Equation T.1 defines the sum of employment (N) and unemployment (u) as the labour force, which is normalised to 1. Equation T.2 outlines employment dynamics and relates employment to hires (h). Equation T.3 defines labour market tightness (θ) as the ratio of vacancies (v) to unemployment. T.4 contains a standard constant returns matching function, while T.5 and T.6 define the vacancy filling rate (q) and the job finding rate (f) respectively. Equation T.7 contains the production function. T.8 defines the marginal cost of hiring labour. Equation T.9 gives the wage, where we have assumed simple Nash bargaining. Equation T.10 defines marginal cost, while T.11 relates price to marginal cost. Equation T.12 is the Euler equation; a summary of these values are in the lower panel of Table 1.

We analyse the impact of four structural shocks. We identify a productivity shock, assuming $A_t = e^{\epsilon_t^P}$. We include a demand shock, ϵ_t^D. We also include a shock to worker relative bargaining power, assuming $z_t = ze^{\epsilon_t^z}$, where ϵ_t^z is a bargaining power shock. And there is a shock to the rate of job destruction, assuming $\tau_t = \tau e^{\epsilon_t^\tau}$, where ϵ_t^τ is a job separations shock. We use impulse response functions to these shocks to impose impact sign restrictions on our structural model.

We specify ranges of values for parameter calibrations and assume that parameters are uniformally distributed within this range. We assume that values of α are uniformally distributed between $0.3 - 0.7$; this is somewhat wider than the range of credible values suggested by Petrongolo and Pissarides (2001). We also consider a wide range of values for matching efficiency, assuming that values of m are uniformally distributed between $0.3 - 1.5$. For the rate of job destruction, Hall and Milgrom (2008) use $\tau = 0.03$, while Pissarides (2009) uses $\tau = 0.036$. These calibrations are designed for monthly data, whereas we use a quarterly frequency, consistent with our data. We therefore consider values between $0.087 - 0.104$. The value of the opportunity cost of employment is also contentious; Shimer (2005) assumes $b = 0.4$, Hall and Milgrom (2008) assume $b = 0.71$. We assume that b is uniformally distributed between 0.4 and 0.8. For the bargaining power of workers, we consider values between $z = 0.1$, so workers have little power to $z = 0.8$, where workers are able to extract most of the surplus from a job match in the form of higher wages. We consider a wide range of values for the probability that prices are fixed, considering values in the range $\theta_\pi = 0$ to $\theta_\pi = 0.9$, encompassing the cases where there is little nominal rigidity and where prices are highly

Table 1: **Contemporaneous Impact of Short-run Shocks on Labour Market Variables**
Notes: Panel a) of this table shows the theoretical model that we simulate. Panel b) shows the range of parameter values from which we sample in our simulations

a) Model Summary

$$N_t + u_t = 1 \tag{T.1}$$

$$N_t = (1 - \tau_t)N_{t-1} + h_{t-1} \tag{T.2}$$

$$\theta_t = \frac{v_t}{u_t} \tag{T.3}$$

$$h_t = m u_t^{\alpha} v_t^{(1-\alpha)} \tag{T.4}$$

$$q_t = m\theta_t^{-\alpha} \tag{T.5}$$

$$f_t = q_t \theta_t \tag{T.6}$$

$$Y_t = A_t N_t \tag{T.7}$$

$$\lambda_t = \frac{\kappa}{q_t} - \beta \mathbb{E}_t \frac{\kappa(1 - \tau_{t+1})}{q_{t+1}} \tag{T.8}$$

$$w_t = (1 - z_t)b + z_t(A_t + \kappa\theta_t) \tag{T.9}$$

$$mc_t = \frac{w_t + \lambda_t}{A_t} \tag{T.10}$$

$$\frac{P_t^*}{P_t} = \frac{\eta}{1 - \eta} (1 - \beta\omega) \mathbb{E}_t \sum_{k=0}^{\infty} (\beta\omega)^k mc_{t+k} \tag{T.11}$$

$$Y_t^{-\eta} = \beta e^{\epsilon_t^D} \mathbb{E}_t Y_{t+1}^{-\eta} \frac{(1 + i_t)}{1 + \pi_{t+1}} \tag{T.12}$$

$$(1 + i_t) = (1 + \pi_t)^{\rho_\pi} \tag{T.13}$$

b) Credible Calibration Ranges

Parameter	Interpretation	Range
β	Discount Factor	0.996
α	Elasticity of Matching wrt Unemployment	$0.3 - 0.7$
m	Efficiency of Job Matching	$0.3 - 1.5$
b	Opportunity Cost of Employment	$0.4 - 0.8$
τ	Rate of Job Destruction	$0.087 - 0.104$
z	Worker Relative Bargaining Power	$0.1 - 0.8$
θ_p	Probability Prices Are Fixed	$0. - 0.9$
ρ_π	Monetary Policy Response to Inflation	$1.35 - 2.0$
η	Intertemporal Elasticity of Substitution	1
κ	Cost of Vacancy Posting	0.2

sticky. For the monetary policy response to inflation, we consider values between $\rho_\pi = 1.35$ and $\rho_\pi = 2.0$, encompassing the different estimated values for this parameter in the post-1979 period. We use $\eta = 1$ and set $\kappa = 0.2$.

We simulate our model by randomly selecting a set of calibration values from the distributions we outline above. We calculate the steady-state solution for our model implied by this calibration and construct impulse responses from a log linear expansion of the model around this steady-state. We repeat this process 1000 times, building a distribution of impulse responses. These distributions are shows in Figures 4)-7). We use these to construct the sign restrictions documented in Table 1) of the main paper. In that table, + indicates that all values for the impulse response on impact within the credible range were positive, − indicates that all values for the impulse response on impact within the credible range were negative, and x indicates that the credible range for the impulse response on impact included zero.

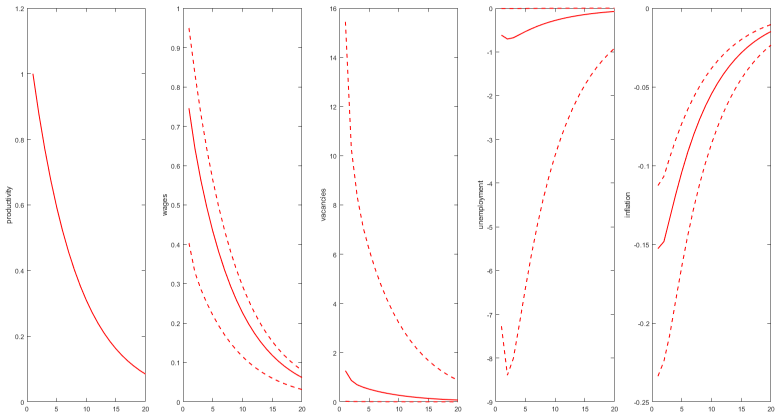

Figure 4: **Median and 10%-90% Bounds of Impulse Responses to Productivity Shocks**
Notes: This figure plots the distribution of impulse response functions following productivity shocks, based on 1000 replications of the model outlined in Table 1 and sampling from the distribution of parameter values outlined in that table.

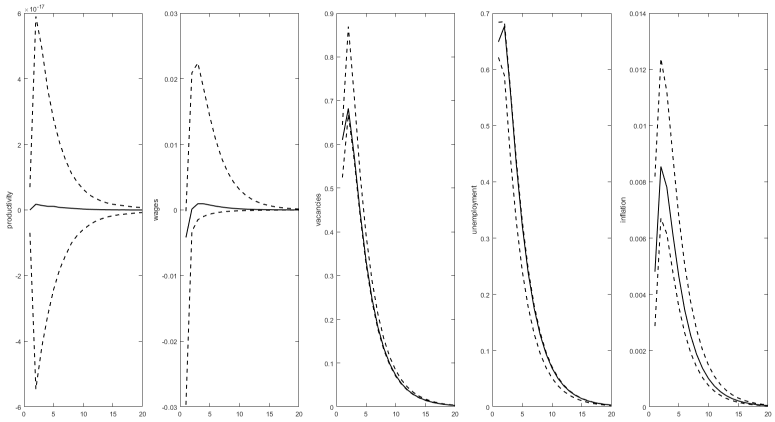

Figure 5: **Median and 10%-90% Bounds of Impulse Responses to Job Separation Shocks**
Notes: This figure plots the distribution of impulse response functions following job separations shocks, based on 1000 replications of the model outlined in Table 1 and sampling from the distribution of parameter values outlined in that table.

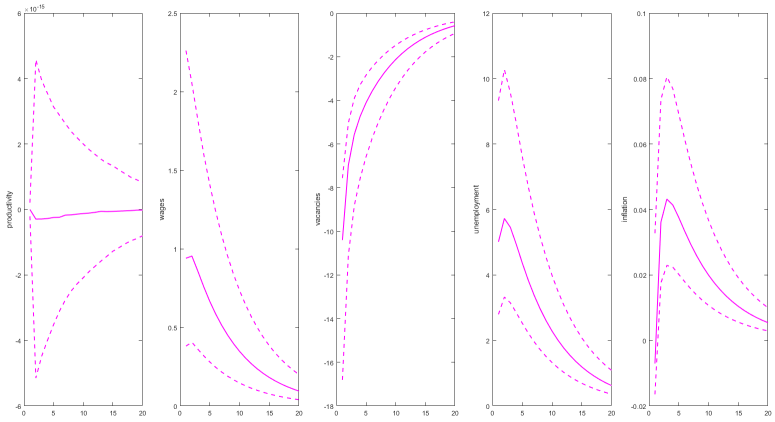

Figure 6: **Median and 10%-90% Bounds of Impulse Responses to Bargaining Power Shocks**
Notes: This figure plots the distribution of impulse response functions following bargaining power shocks, based on 1000 replications of the model outlined in Table 1 and sampling from the distribution of parameter values outlined in that table.

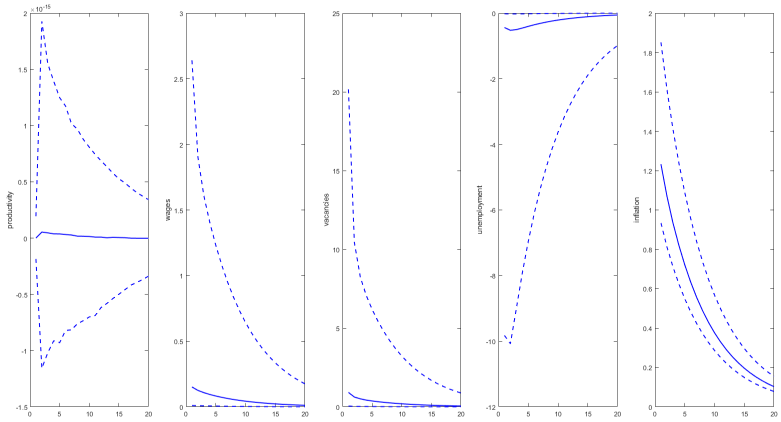

Figure 7: **Median and 10%-90% Bounds of Impulse Responses to Demand Shocks**
Notes: This figure plots the distribution of impulse response functions following demand shocks, based on 1000 replications of the model outlined in Table 1 and sampling from the distribution of parameter values outlined in that table.

5 Robustness Analysis

5.1 An Alternative Productivity Series

To assess the robustness of our main findings, we now replace our original productivity series with that of Fernald (2014). We re-run our baseline model exactly as before and implement the same sign restrictions. Figures 8 and 9 report our results analogous to Figures 1 and 2 in the main text.

Overall, it is clear that replacing our original productivity series with that of Fernald (2014) yields qualitatively similar conclusions to those we report in the main text. Productivity and wage bargaining shocks account for the majority of wage and unemployment variation with an increasing relative importance of wage bargaining shocks as we move through our sample. This provides further evidence supporting Fujita and Ramey (2007), Theodoridis and Zanetti (2020), Drautzburg et al. (2021) and Ellington et al. (2021). We can also see that while the average semi elasticity across all shocks remains stable over the sample, the absolute value of the semi-elasticity in response to productivity shocks has risen.

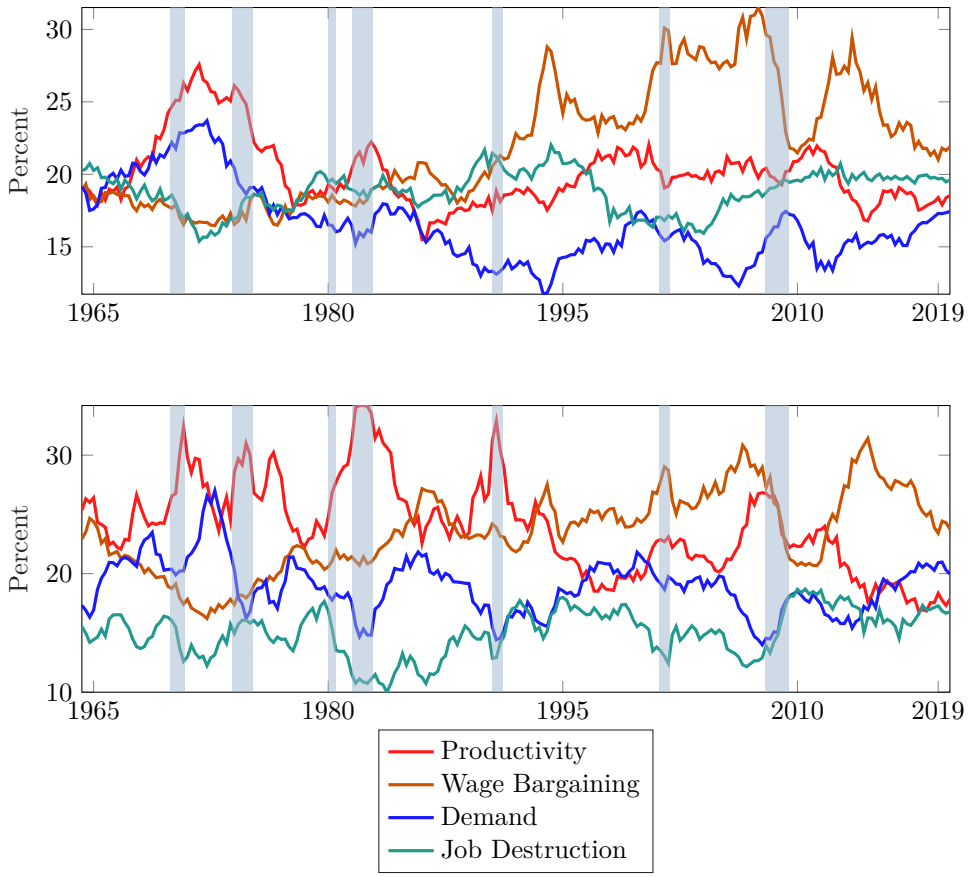

Figure 8: **Variance Decomposition of Wages and Unemployment using Fernald (2014) Productivity**
Notes: This figure plots the contribution of (i) productivity shocks (red); (ii) wage bargaining power shocks (brown); (iii) demand shocks (blue) and (iv) job destruction shocks (green) in explaining the 1-period ahead variation in wages (top panel) and unemployment (lower panel) across our sample.

5.2 An Alternative Identification Strategy

We now focus on an alternative empirical identification strategy. We combine the maximum forecast error variance procedure of Uhlig (2004) with our sign restrictions that stem from the theoretical model. This is in a similar vein to Pizzinelli et al. (2020). In doing so, we impose the restriction that the productivity shock explains the majority of the forecast error variance of labour productivity at business cycle frequencies (i.e. from horizons 0 to 40)[1]. To ease computational burden because we have a TVP VAR model, we compute simple impulse responses and sample every fourth quarter. Figures 10 and 11 report our results analogous to Figures 1 and 2 in the main text.

Again on the whole, using an alternative identification scheme results in similar conclusions to our baseline analysis. Productivity and wage bargaining shocks account for the majority of wage and unemployment variation with an increasing relative importance of wage bargaining shocks as we move through our sample. However, note that the absolute value of the forecast error variance

[1]For technical details on this procedure, see Appendix B.2 in Pizzinelli et al. (2020).

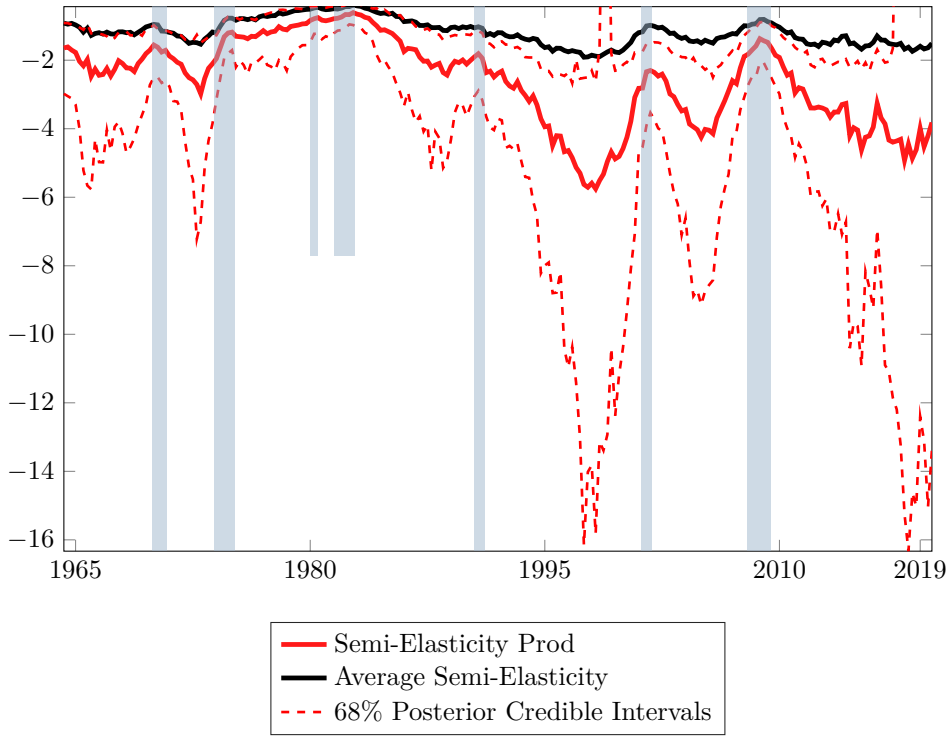

Figure 9: **Variation in Estimated Semi-Elasticities Over Time using Fernald (2014) Productivity**

Notes: This figure plots estimated semi-elasticities of real wages with respect to unemployment, calculated as the ratios of the estimated impulse response functions, using $k = 1$. The figure plots (i) the estimated semi-elasticity of wages with respect to unemployment following productivity shocks (red), with associated credibility bands; (ii) the estimated semi-elasticity of wages with respect to unemployment averaged across all shocks using forecast error variance decompositions to weight shocks.

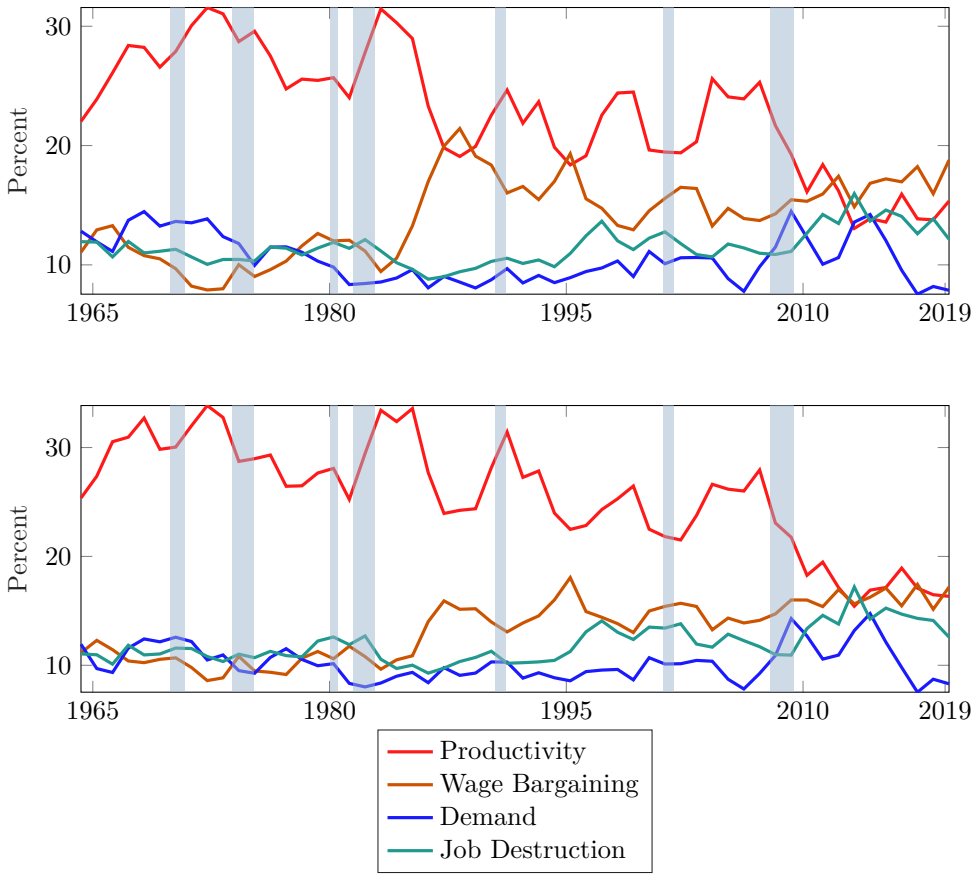

Figure 10: **Variance Decomposition of Wages and Unemployment; An Alternative Identification Scheme**

Notes: This figure plots the contribution of (i) productivity shocks (red); (ii) wage bargaining power shocks (brown); (iii) demand shocks (blue) and (iv) job destruction shocks (green) in explaining the 1-period ahead variation in wages (top panel) and unemployment (lower panel) across our sample.

shares associated to wage bargaining shocks is slightly lower than our baseline analysis. Turning to the semi-elasticity plots in Figure 11 it is clear that the absolute value of the semi-elasticity in response to productivity shocks has risen throughout the sample while the semi-elasticity averaged over all shocks remains relatively stable.

In general these robustness checks further substantiate our main findings and provides additional empirical evidence that one cannot attribute unemployment volatility to real wage rigidity.

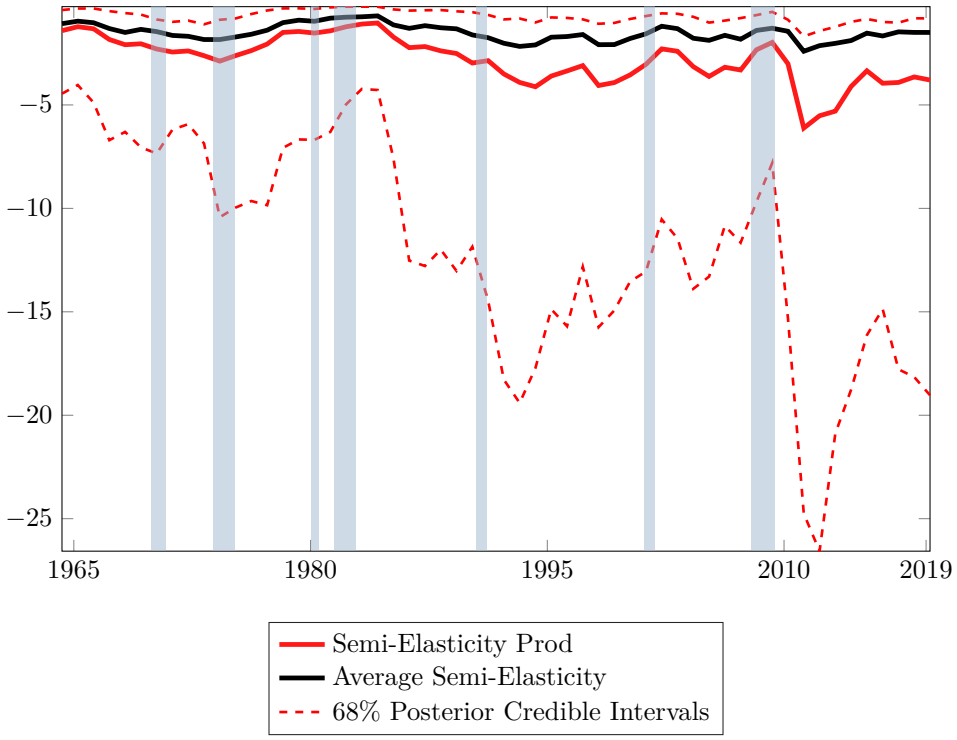

Figure 11: **Variation in Estimated Semi-Elasticities Over Time; An Alternative Identification Scheme**

Notes: This figure plots estimated semi-elasticities of real wages with respect to unemployment, calculated as the ratios of the estimated impulse response functions, using $k = 1$. The figure plots (i) the estimated semi-elasticity of wages with respect to unemployment following productivity shocks (red), with associated credibility bands; (ii) the estimated semi-elasticity of wages with respect to unemployment averaged across all shocks using forecast error variance decompositions to weight shocks.

6 Alternative Calibrations

In this section we explore the consequences of differing values for wage rigidity for macroeconomic modelling. We calibrate a workhorse New Keynesian model with matching frictions in two scenarios. In the first, we calibrate the model in order to match the value for the wage rigidity in response to productivity shocks that we use in the current literature. In the other, we calibrate in order to match the smaller value of wage rigidity that we find in this paper.

To do this, we use the model outlined and used to derive credible sign restrictions, in section 4). We set $\alpha = 0.5$, $m = 1.7$, $\tau = 0.1$, $\theta_p = 0.5$, $\rho_\pi = 1.5$ and $\eta = 1$. We also target an unemployment rate of 5.2%. Given these, we solve for the values of w, κ and λ that satisfy (T.8)-(T.10) in Table 1) above and calibrate z and b to give the desired value of the semi-elasticty of wages with respect to unemployment. In secenario 1), we target a semi-elasticity of wages with respect to productivity shocks of $se^{\text{Prod}}_{t+1,t} = -0.46$, the value obtained by Gertler et al (2020); in scenario 2), we target $se^{\text{Prod}}_{t+1,t} = -2.17$. For scenario 1), we obtain $b = 0.71$, and $z = 0.085$; for scenario 2), we obtain $b = 0.4$ and $z = 0.88$.

Table 2: **Simulation Results**

Parameter	Interpretation	Scenario 1	Scenario 2
σ_u	Volatility of Unemployment	0.031	0.01
σ_w	Volatility of the Wage	0.014	0.02
$\rho_{w,u}$	Correlation Between Wage and Unemployment	-0.987	-0.983
ψ_w	First-Order Autocorrelation of the Wage	0.878	0.878
ψ_u	First-Order Autocorrelation of unemployment	0.935	0.935

Our results are summarised in Table 2). As we might expect, the volatility of unemployment relative to the volatility of wages is higher with the values of real wage rigidity used in the existing literature which are reflected in Scenario 1), compared to our estimated lower value for real wage rigidity, reflected in Scenario 2). Although our simple DSGE model is not designed to replicate the high value of unemployment volatility that is observed in the data, it is clear that our finding of a low value for wage rigidity challenges existing models that are able to generate a high value for unemployment volatility.

To explore this further, we used a calibration similar to that of Hagedorn and Manovskii (2008), a well-known paper that is able to generate a large volatility of unemployment. In particular, we set $b = 0.955$ and $z = 0.052$. The resultant semi-elasticity of wages with respect to unemployment is only -0.05, much lower than any estimate in the literature. We also used a calibration similar to that of Shimer (2005), whose calibration does not generate a large unemployment volatility. In this case, we set $b = 0.4$ and $z = 0.72$; the resultant semi-elasticity is -1.56, which is consistent with existing evidence, although somewhat lower than our estimate. These experiments highlight how our results create a challenge to the theoretical literature, since it is not clear whether any existing model can match the high value of unemployment volatility in the data while also matching the small value for real wage rigidity that we estimate in this paper.

References

Canova, F. and Paustian, M. (2011), 'Business cycle measurement with some theory', *Journal of Monetary Economics* **58**(4), 345–361.

Cogley, T. and Sargent, T. J. (2005), 'Drifts and Volatilities: Monetary Policies and Outcomes in the post WWII US', *Review of Economic Dynamics* **8**(2), 262–302.

Doan, T., Litterman, R. and Sims, C. (1984), 'Forecasting and Conditional Projection using Realistic Prior Distributions', *Econometric Reviews* **3**(1), 1–100.

Drautzburg, T., Fernández-Villaverde, J. and Guerrón-Quintana, P. (2021), 'Bargaining Shocks and Aggregate Fluctuations', *Journal of Economic Dynamics and Control* **127**, 104121.

Ellington, M., Martin, C. and Wang, B. (2021), 'Search Frictions and Evolving Labour Market Dynamics', *Journal of Economic Dynamics and Control* .

Fernald, J. (2014), 'A quarterly, utilization-adjusted series on total factor productivity', *Federal Reserve Bank of San Francisco Working Paper 2012-19* .

Fujita, S. and Ramey, V. (2007), 'Exogenous versus endogenous separation', *American Economic Journal: Macroeconomics* **4**(4), 68–93.

Hall, R. E. and Milgrom, P. R. (2008), 'The Limited Influence of Unemployment on the Wage Bargain', *American Economic Review* **98**(4), 1653–74.

Hamilton, J. D. (2018), 'Why You Should Never use the Hodrick-Prescott Filter', *Review of Economics and Statistics* **100**(5), 831–843.

Jacquier, E., Polson, N. G. and Rossi, P. E. (2002), 'Bayesian Analysis of Stochastic Volatility Models', *Journal of Business & Economic Statistics* **20**(1), 69–87.

Koop, G. and Korobilis, D. (2010), *Bayesian Multivariate Time Series Methods for Empirical Macroeconomics*, Now Publishers Inc.

Litterman, R. B. (1986), 'Forecasting with Bayesian Vector Autoregressions—Five Years of Experience', *Journal of Business & Economic Statistics* **4**(1), 25–38.

Mumtaz, H. and Zanetti, F. (2012), 'Neutral technology shocks and the dynamics of labor input: Results from an agnostic identification', *International Economic Review* **53**(1), 235–254.

Mumtaz, H. and Zanetti, F. (2015), 'Labor Market Dynamics: A Time-varying Analysis', *Oxford Bulletin of Economics and Statistics* **77**(3), 319–338.

Pissarides, C. A. (2009), 'The Unemployment Volatility Puzzle: Is Wage Stickiness the Answer?', *Econometrica* **77**(5), 1339–1369.

Pizzinelli, C., Theodoridis, K. and Zanetti, F. (2020), 'State dependence in labor market fluctuations', *International Economic Review* **61**(3), 1027–1072.

Primiceri, G. E. (2005), 'Time-varying Structural Vector Autoregressions and Monetary Policy', *Review of Economic Studies* **72**(3), 821–852.

Shimer, R. (2005), 'The Cyclical Behavior of Equilibrium Unemployment and Vacancies', *American Economic Review* **95**(1), 25–49.

Theodoridis, C. P. K. and Zanetti, F. (2020), 'State dependence in labor market fluctuations: Evidence, theory, and policy implications', *Journal of Economic Dynamics and Control* **61**(3), 1027–72.

Uhlig, H. (2004), 'Do technology shocks lead to a fall in total hours worked?', *Journal of the European Economic Association* **2**(2-3), 361–371.